Received: 28 May 2019 | Revised: 11 July 2019 | Accepted: 14 July 2019

DOI: 10.1002/arch.21608

RESEARCH ARTICLE

Archives of INSECT BIOCHEMISTRY AND PHYSIOLOGY WILEY

Knockdown of arylalkylamine *N*-acetyltransferase-like 2 in *Drosophila melanogaster*

Ryan L. Anderson | Dylan J. Wallis | Alexander Aguirre | Dean Holliday | David J. Merkler

Department of Chemistry, University of South Florida, Tampa, Florida

Correspondence
David J. Merkler, Department of Chemistry, University of South Florida, 4202 E. Fowler Ave. CHE 205, Tampa, FL 33620.
Email: merkler@usf.edu

Funding information
National Institute of Drug Abuse at the National Institutes of Health, Grant/Award Number: R03 DA034323; National Institute of General Medical Science of the National Institutes of Health, Grant/Award Number: R15-GM107864; University of South Florida, Grant/Award Number: Creative Scholarship Grant from the College of Art; Shirley W. and William L. Griffin Charitable Foundation

Abstract

Drosophila melanogaster produces fatty acid amides, and thus, provides a model to unravel the pathways for their biosynthesis. We previously demonstrated that arylalkylamine *N*-acetyltransferase-like 2 (AANATL2) from *D. melanogaster* will catalyze the formation of long-chain *N*-acylserotonins and *N*-acyldopamines in vitro. Generating silencing RNA via the UAS/GAL4 bipartite approach for targeted gene expression effectively decreased the endogenous levels of the AANATL2 transcripts in *D. melanogaster*, as shown by reverse transcription quantitative polymerase chain reaction. Consistent with these data, western blot analysis of the offspring of the AANATL2 knockdown flies using an anti-AANATL2 antibody revealed a significant reduction in the expression of the AANATL2 protein. Reduced expression of AANATL2 decreased the cellular levels of *N*-palmitoyldopamine (PALDA), providing strong evidence that AANATL2 is responsible for the biosynthesis of PALDA in vivo. This is the first time

Abbreviations: AANATL2, aryalkylamine *N*-acetyltransferase-like 2; CB, cannabinoid receptor; LC-QToF-MS, liquid chromatography time-of-flight mass spectrometry; PALDA, *N*-palmitoyldopamine; siRNA, silencing RNA; ssRNA, single-stranded RNA; UAS, upstream activator sequence.

Present address Ryan L. Anderson, Department of Biochemistry and Molecular Genetics, University of Colorado, Denver Anschutz Medical Campus, Aurora, CO.

Dylan J. Wallis, Toxicology Program, Department of Biological Sciences, Bioinformatics Research Center, North Carolina State University, Raleigh, NC 27695.

Dean Holliday, USF Morsani College of Medicine, University of South Florida, 12901 Bruce B. Downs Blvd., Tampa, FL 33612.

that the expression of an AANAT has been reduced in *D. melanogaster* to link one of these enzymes to the in vivo production of an *N*-acylarylalkylamide.

KEYWORDS
arylalkylamine *N*-acetyltransferase, *Drosophila melanogaster*, expression knockdown, fatty acid amide, LC-QToF-MS, *N*-palmitoyldopamine, UAS/Gal4

1 | INTRODUCTION

Endocannabinoids are a family of compounds originating from the discovery of the mammalian cannabinoid receptors, CB_1 and CB_2, and anandamide (*N*-arachidonoylethanolamide) the endogenous ligand for CB_1 (Devane, Dysarz, Johnson, Melvin, & Howlett, 1988; Devane et al., 1992; Munro, Thomas, & Abu-Shaar, 1993). The two best understood endocannabinoids are anandamide and 2-arachidonoylglycerol (Devane et al., 1992; Mechoulam et al., 1995; Sugiura et al., 1995). We have had a longstanding interest in the lipids structurally related to anandamide, the fatty acid amide (FAA), R–CO–NH–R′ (R–CO– is derived from a fatty acid and –NH–R′ is derived from a biogenic amine). The endocannabinoid-like FAAs are subdivided into the *N*-acylethanolamines, *N*-acylamino acids, *N*-acylarylalkylamides, and primary FAAs. These molecules are of biological significance because they likely serve a myriad of functions in vertebrates and in invertebrates, from sleep induction in mammals to cuticle sclerotization in insects (Bradshaw, Lee, & McHugh, 2009; Iannotti, Di Marzo, & Petrosino, 2016; Witkamp, 2016). Despite their potential importance and broad occurrence in living systems, much remains unknown about several FAAs, including definitive evidence for their functions in vivo, the receptors and other proteins to which these bind, and how these are derived from dietary fats (Bradshaw et al., 2009; Iannotti et al., 2016; Merkler & Leahy, 2018). The identification of FAAs in insects (Alborn et al., 1997; Anderson et al., 2018; Fezza et al., 2003; Jeffries, Dempsey, Behari, Anderson, & Merkler, 2014; Tortoriello et al., 2013; Yoshinaga et al., 2007) is intriguing because insects do not express orthologs to the mammalian CBs (Elphick, Satou, & Satoh, 2003; McPartland, Di Marzo, De Petrocellis, Mercer, & Glass, 2001). One of our concerns regarding FAAs is the enzyme responsible for their biosynthesis. One possible route to the FAAs in vivo would be a reaction between an amine, like serotonin or dopamine, and a fatty acyl-CoA: R–CO–S–CoA + H_2N–R′ → R–CO–NH–R′ + CoA–SH. Enzymes in the GNAT superfamily of *N*-acetyltransferases catalyze a similar reaction utilizing acetyl-CoA as the acyl-CoA donor to generate *N*-acetylamines (Ud-Din, Tikhomirova, & Roujeinikova, 2016; Vetting et al., 2005). *Drosophila melanogaster* produces FAAs (Jeffries et al., 2014; Tortoriello et al., 2013; Yoshinaga et al., 2007) and expresses a number of *N*-acetyl and *N*-acyltransferases (O'Flynn, Suarez, Hawley, & Merkler, 2018). Thus, *D. melanogaster* is a valuable model organism for the study of FAA biosynthesis. We have identified and characterized a *D. melanogaster N*-acyltransferase, arylalkylamine *N*-acetyltransferase-like 2 (AANATL2), which catalyzes the formation of *N*-fatty acyldopamines and serotonins in vitro (Dempsey et al., 2014; Dempsey, Carpenter, Ospina, & Merkler, 2015). While this enzyme is formally named an *N*-acetyltransferase, we have shown that AANATL2 will accept long-chain acyl-CoAs as substrates (Dempsey et al., 2014), and thus, AANATL2 should be considered an *N*-acyltransferase. Transcripts for AANATL2 are found at substantially higher levels in the thorax-abdomen of *D. melanogaster* and *N*-fatty acylserotonins were identified only in the thorax-abdomen of *D. melanogaster* (Amherd, Hintermann, Walz, Affolter, & Meyer, 2000; Dempsey et al., 2014). In aggregate, these data suggest, but do not prove, that AANATL2 is responsible for the in vivo production of the *N*-fatty acylserotonins and *N*-fatty acyldopamines in *D. melanogaster*.

Herein, we report on the knockdown of AANATL2 expression in *D. melanogaster* using the UAS/Gal4 bipartite system (Brand & Perrimon, 1993; Duffy, 2002; Giniger, Varnum, & Ptashne, 1985; Kalidas & Smith, 2002). Knockdown of AANATL2 of 80–85% results in viable offspring that produces no detectable levels of *N*-palmitoyldopamine (PALDA), increased levels of other *N*-palmitoylated amines, and a ~10-fold increase in oleamide. These data are consistent with

the in vitro substrate specificity of AANATL2 and suggest that AANATL2 is responsible for biosynthesis of *N*-fatty acyldopamines in the fruit fly. These results from *D. melanogaster* may have broader significance because *N*-fatty acyldopamines are found in the plasma and striatum of mammals (Chu et al., 2003; Hauer et al., 2013; Walker et al., 2005), but the enzyme responsible for their biosynthesis in mammals is currently unknown.

2 | MATERIALS AND METHODS

2.1 | General care of fly stocks

Drosophila upstream activator sequence (UAS) stocks (CG9486) were purchased from Vienna *Drosophila* Resource Center and were homozygous for an AANTAL2 silencing RNA (siRNA) hairpin that was transposed into the second chromosome. The Gal4 drivers were purchased from Bloomington Labs (5138) and exhibited the ubiquitous expression of Gal4 and a balancer chromosome (inserted into the third chromosome) containing the stubble (Sb[1]) phenotype. Both strains were cultured on Instant *Drosophila* Medium from Carolina Biological in *Drosophila* vials capped with BuzzPlugs™ from Thermo Fisher Scientific.

2.2 | UAS/Gal4 crossing scheme to generate *AANATL2* knockdown flies

The Gal4 drivers were all female in the crossing scheme to reduce the collection of false-positive offspring. Males for the cross were from the UAS flies. The Gal4 adult flies were first split into new culturing tubes, procreated, and then laid eggs for 7 days. After this period, all adults were removed from the culturing tubes, leaving the larvae behind. The larvae could then enter pupation and were closely monitored. Once the newly hatched flies began to emerge, virgin female Gal4 drivers were swiftly collected in the afternoon using FlyNap and a low-powered magnification microscope. Virgin females were collected based on the positive identification of the appropriate size, banding pattern, and presence of the meconium. Five virgin females were placed into freshly prepared tubes, to which five anesthetized UAS males were added. The UAS males and Gal4 females were left for 5 days before being separated into new vials. Once the offspring of the cross hatched, AANATL2 knockdown flies were chosen based on the negative appearance of the stubble gene (Sb[1]; Figure 1) using our same established methods for virgin females. Collected flies were flash frozen in liquid N_2 and stored at −80°C until needed. UAS flies were placed in culture tubes on ice, poured into a conical vial to separate the adults from larvae and media, flash frozen in liquid N_2, and the frozen flies were stored in a −80°C ultrafreezer.

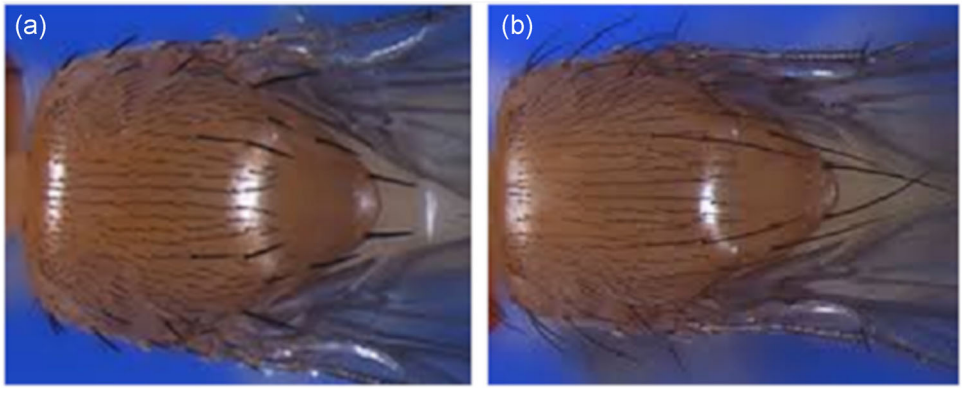

FIGURE 1 Matching *m/z* and retention times of fatty acid amides detected in the thorax-abdomen of *Drosophila melanogaster* exhibiting the stubble (Sb[1]) phenotype from the balancer chromosomes. (b) Shows the dorsal thorax of an AANATL2 knockdown *D. melanogaster*, note the difference in the length of the bristles between (a) (shorter) and (b) (longer). AANATL2, arylalkylamine *N*-acetyltransferase-like 2

TABLE 1 Primer design for *Drosophila* AANATL2 and Actin-42A

Targets	Forward primer	Reverse primer	Product size (bp)
AANATL2	CATACGCGCCATGACAATC	GACACCTCGCTCTGCTTG	120
Actin-42A	CACAGGTATCGTGTTGGACTC	AGGTAGTCGGTTAAATCGCG	123

Abbreviation: AANATL2, arylalkylamine *N*-acetyltransferase-like 2.

2.3 | Detection of *AANATL2* transcripts via reverse transcription quantitative polymerase chain reaction (RT-qPCR)

AANATL2 qPCR primers were designed to amplify 75-150 bp regions of the open reading frame of the target *AANATL2* and an endogenous control (Table 1). Actin-42A was chosen as an endogenous control for qPCR. Primer sequences were generated using Integrated DNA Technologies and were designed to prevent the formation of primer dimers, or a hairpin, and to have an annealing temperature of approximately 60°C. Primers were targeted to the 5′-end of the messenger RNA (mRNA), as it was previously found that primer designations closer to the 3′-end had the possibility of not showing mRNA degradation. This was due to the possibility of there remaining dicer-degraded fragments of sufficient length for PCR amplification (Holmes, Williams, Chapman, & Cross, 2010).

Stocks of mRNA were gathered in the same manner for both the UAS parent and knockdown offspring. Dempsey et al. (2014) discovered that *AANATL2* transcripts were concentrated in the thorax-abdomen of *D. melanogaster*. For this reason, flies were collected, flash frozen in liquid N_2, shaken vigorously to detach the head from the thorax-abdomen, and the body segments were segregated using a sieve. Total RNA was extracted from 200 mg of thorax-abdomen using TRIzol, and the resulting RNA collected using a Pure Link RNA Minikit (Invitrogen). The mRNA was isolated using PolyA-Tract (Promega) and concentrated using a 10 kDa spin ultrafilter. Genomic DNA was removed using DNase I from Invitrogen with the following modifications to the manufacturer's protocol: 2 µl of DNase I, $MgCl_2$ buffer, and ethylenediaminetetraacetic acid (EDTA) were used per 1 µg of mRNA. All purified mRNA stocks were stored at −20°C as 10 ng/µl solutions. The qPCR reactions (Table 2) were set up on a 96-well plate using mRNA from either the UAS parent or AANATL2 knockdown offspring.

All qPCR experiments were setup for $\Delta\Delta C_T$ analysis and carried out on an Applied Biosystems QuantStudio 3 (Thermo Fisher Scientific) using the SYBR Green Mastermix. The first step of heating was a hold at 50°C for 45 min for the creation of complementary DNA (cDNA) by reverse transcriptase. The temperature was then held at 95°C for 10 min to inactivate the reverse transcriptase. Subsequent PCR thermal cycles were as follows: 95°C for 15 s and then a decrease of 1.6°C/s to hold at 60°C for 1 min. This method was repeated for 40 cycles. Melting curves were completed using the same cycling temperatures, times, and rates as the PCR cycling.

TABLE 2 Quantitative polymerase chain reactions on a 96-well plate

Sample	mRNA (ng)	SYBR[a] (µl)	Actin-F[b] (nM)	Actin-R[c] (nM)	AANATL2-F[d] (nM)	AANATL2-R[e] (nM)	RT (U)	Water[f] (µl)
UAS[g]	30 ng	10	200	200	200	100	40	to 20
KD[h]	30 ng	10	200	200	200	100	40	to 20

Abbreviations: AANATL2, aryalkylamine *N*-acetyltransferase-like 2; KD, knockdown; mRNA, messenger RNA; RT, reverse transcriptase; UAS, upstream activator sequence.
[a]Power Up SYBR Green from Thermo Fisher Scientific.
[b]Forward primer for actin.
[c]Reverse primer for actin.
[d]Forward primer for *AANATL2*.
[e]Reverse primer for *AANATL2*.
[f]Nuclease-free water.
[g]UAS parent.
[h]AANATL2 knockdown offspring.

The resulting qPCR amplicons were evaluated by electrophoresis and sequenced to assure amplification of the authentic *AANATL2* transcripts. An aliquot (40 μl) of the qPCR amplicon was taken from the 96-well plate, combined with 10 μl of purple loading dye (NEB), and loaded onto a 1.8% agarose gel with 127 nM ethidium bromide. Electrophoresis was run for 1.5 hr at 50 V, DNA bands were visualized with ultraviolet light, and amplicons of the appropriate, matching size were cut out of the gel with a clean razor blade. DNA was extracted from the agarose gel slices using the Wizard SV Gel and PCR Clean-up System (Promega) and sequenced commercially by Eurofins Genomics.

2.4 | Detection of AANATL2 protein via sodium dodecyl sulfate polyacrylamide gel electrophoresis (SDS-PAGE)/western blot analysis

Proteins were collected from the UAS parent and knockdown offspring, separately, in the following way: 5 ml of a lysis buffer was made by combining 2,500 μl 2× lysis solution (40 mM Tris-HCl, pH 7.4, 4 mM $MgCl_2$, 2 mM EDTA, 2 mM ethylene glycol-bis(β-aminoethyl ether)-*N*,*N*,*N*′,*N*′-tetraacetic acid, 300 mM NaCl, and 2.0% Triton X-100), 300 μl protease inhibitor cocktail (catalog no.: P8340; Sigma-Aldrich), 25 μl (200 mM) of phenylmethylsulfonyl fluoride, 50 μl (100 mM) of Na_3VO_4, and 2,125 μl of water. All protease inhibitors were prepared fresh before lysis. Approximately 20 flash-frozen thorax-abdomen were prepared and collected using the method described in Section 2.3. These were placed into 5 ml of lysis buffer in a mortar and pestle and the mixture ground to lyse the cells. The homogenate was pipetted into a vial, sonicated for 3 min (30 s pulses with 30 s of rest) on ice, and centrifuged at 13,400 rpm for 5 min. The resulting supernatant containing the cellular proteins was collected and the pellet discarded. The supernatant was placed into a microcentrifuge tube on ice, transferred to a 10 kDa spin ultrafilter, and centrifuged at maximum speed to concentrate the proteins with a molecular weight >10 kDa. The protein concentration of the supernatant was measured using the Bradford dye-binding assay (Bradford, 1976). A volume containing 22 μg of protein was added to an equal volume of 2× Laemmli Buffer containing β-mercaptoethanol and the solution placed into a 100°C water bath for 3 min to denature the proteins. The proteins were separated by 15% SDS-PAGE after the addition of a Bio-Rad color marker set (7 μl; New England Biolabs), Magic Marker (5 μl; New Enlgand Biolabs), and 5 ng of pure, recombinant *D. melanogaster* AANATL2 with an N-terminal His_6-tag. The recombinant *D. melanogaster* His_6-AANATL2 was a gift from Dr. Daniel R. Dempsey. After completing the SDS-PAGE protein separation, the proteins within the gel were transferred to a nitrocellulose membrane using the sandwich method. The assembled sandwich was inserted into the appropriate cassette and then placed into an electrophoresis transfer apparatus holding transfer buffer (25 mM Tris-base, 192 mM glycine, and 10% methanol). Electrophoresis was completed at 4°C while stirring at 100 V for approximately 1 hr. The nitrocellulose membrane was removed from the apparatus, washed in TBST (20 mM Tris, 500 mM NaCl, and 20 μl of Tween), placed into a solution containing 2.0 g of nonfat dry milk in 40 ml TBST, and gently rocked for 2 hr. The membrane was washed in TBST and cut horizontally at the 40 kDa molecular weight marker. The top half of the membrane was placed into a solution containing 25 μg/ml rabbit anti-*Drosophila* α-tubulin polyclonal antibody (pAb; Santa Cruz Biotech) in 40 ml TBST, while the bottom half was placed into a separate solution containing 0.5 μg/ml rabbit anti-*D. melanogaster* AANATL2 pAb (custom synthesized by Genscript) in 40 ml TBST. Both solutions were rocked overnight at 4°C. Each half of the nitrocellulose was washed with TBST and transferred into separate containers with identical solutions of 0.5 μg/ml goat antirabbit immunoglobulin G-horseradish peroxidase (HRP) conjugate (as the secondary antibody) in 40 ml TBST, and rocked at room temperature for 2 hr. Each half was placed into separate solutions containing 10 ml HRP substrate (stable peroxide/enhancer solution, 1:1) and was allowed to sit for 5 min while rocking gently. Membrane halves were removed, dried completely, and the dried halves aligned together, exposed, and developed. The X-ray film was exposed to the irradiating membrane for 10 min in a dark room and immediately developed.

2.5 | Liquid extraction and purification of lipids from *Drosophila* thorax-abdomen

Frozen thorax-abdomen (0.4 g) from both the UAS parent and AANATL2 knockdown offspring were collected separately in triplicate samples (1.2 g total for each variety of fly, six samples total) and all replicates were treated using the procedures of Sultana and Johnson (2006). Each replicate was dissolved in 14 ml of high-performance liquid chromatography (HPLC) grade methanol and transferred to a mortar and pestle. A solvent blank containing 14 ml of methanol was also prepared and treated in the exact same manner as all *Drosophila* samples. The thorax-abdomen were ground in methanol for 5 min and transferred to a 25 ml vial placed on ice. The remaining, loose collection of fly bodies were sonicated for 15 min on ice to further lyse the cells and expose the lipids in solution. Homogenates were centrifuged for 10 min and the supernatants were collected into a large test tube and capped. Cell pellets were resuspended in 14 ml chloroform/methanol/water (1:1:0.1, v/v/v) and sonicated for 10 min. Supernatants were collected and compiled onto the methanol extracts in the same test tube of the appropriate sample. Cell pellets were reconstituted in 14 ml chloroform/methanol (2:1, v/v) and 2.4 ml (0.5 M) of KCl, 0.08 M phosphoric acid (aq.) was added to create an emulsion. Homogenates were sonicated for 2 min, briefly vortexed, and centrifuged for 10 min. The bottom chloroform-containing organic layer was consolidated into the same test tube as before, with all three solvent types now containing biomaterial from the same type of thorax-abdomen. All extracts were dried under N_2, overnight in a sand bath at 40°C.

Dried extracts were reconstituted in 1 ml *n*-hexane (HPLC-grade). The sides of the tube were thoroughly washed to capture all the organic materials, and the resulting solution transferred to a new, small test tube, ensuring leaving most of insoluble material behind. This process was repeated with another 1 ml of *n*-hexane ,and it was placed into the same, small test tube. The *n*-hexane crude extracts were dried under N_2 at 40°C. DSC-silica (500 mg; Sigma-Aldrich) was placed into a 5 ml drip column and analytical grade sand was placed atop the silica in an approximately 0.3 cm layer. The dried extracts were suspended in 150 µl *n*-hexane, while the silica was equilibrating in 5 ml *n*-hexane. Once the bottom of the meniscus of the equilibrant reached the top of the sand, the entire dissolved extract was injected onto the silica/sand bed and allowed to fully adsorb into the adsorbent. *n*-Hexane (4 ml) was added and dripped into a waste container. The solvent level was allowed to completely enter the resin, without drying out the column, before adding a new solvent, while the flow continued to be directed to the waste. This was continued for the following solvents after *n*-hexane: 1 ml *n*-hexane/acetic acid (99:1, v/v), 1 ml *n*-hexane/ethyl acetate (90:10, v/v), and 1 ml *n*-hexane/ethyl acetate (80:20, v/v). After the 80:20 solvent had almost finished eluting, 1 ml *n*-hexane/ethyl acetate (70:30, v/v) was added, and the resulting eluent was collected into a small test tube. Next, the column was washed and fractions collected in the same tube using the following solvents in this order: 1.5 ml chloroform/2-propanol (2:1, v/v) then 1 ml HPLC-grade methanol. The collected fractions, all in one tube, were capped, and then dried under N_2 at 40°C.

2.6 | Liquid chromatography quadrupole time-of-flight tandem mass spectrometry (LC-QToF-MS/MS) detection of FAAs from *Drosophila* thorax-abdomen

Purified extracts were dissolved in 90 µl methanol/acetonitrile (1:1, v/v), 50 pmole of *N*-arachidonoyldopamine and 50 pmole of *N*-arachidonoylserotonin were added to bring the total volume to 100 µl, and this was transferred to the appropriate insert of a clear 12 × 32 mm vial. These two compounds were chosen as internal standards because they were not detected in an initial pilot experiment containing 0.4 g of fruit fly thorax-abdomen from either the UAS or knockdown lines. A 25 µl aliquot was injected into an Agilent 6540 LC/QToF-MS in positive ion mode and a cutoff of 3,200 *m/z*. A Kinetix 2.6 µm C_{18} 100 Å (50 × 2.1 mm) reverse phase column was used for the separation of lipid extracts from both the UAS parent and AANATL2 knockdown offspring. Mobile phase A was 0.1% formic acid in water, while mobile phase B was 0.1% formic acid in acetonitrile and the flow rate was set to 0.6 ml/min. The elution profile is as follows: linear increase from 10% to 100% B in 5 min and a hold for 3 min at 100% B. The column was then re-equilibrated with 10% B for 8 min after each run. In addition, a wash step was completed after

each run, which was identical to the method just stated, except there was a 50 µl injection and the flow rate was 1.0 ml/min until the equilibration step was reached. The retention time and *m/z* of FAAs were found by matching these to pure standard solutions of the compound and the intensity recorded for each compound found to match. The instrument was calibrated to collect specific FAAs based on their *m/z* and retention time values and to fragment each compound with a collision energy of 15–20 mV. The resulting mass spectra were then analyzed to find the precursor ion and fragments indicative of that specific FAA.

The blank run for each extraction was also scanned for any matching lipids as well. Any quantifiable *m/z* found in the blank were subtracted from each sample replicate to reduce the likelihood of false positives. Once a compound was confirmed based on matching *m/z* and retention time to the standard, the FAA was quantified using standard curves generated from standards ranging from 5 to 500 nM. The average intensity recorded by the mass spectrometer was converted into pmole for each compound detected in each replicate. *N*-Arachidonoylserotonin (50 pmole) and *N*-arachidonoyldopamine (50 pmole) were spiked into each sample before LC-QToF-MS injection, which was used as an internal standard to normalize FAA quantification between replicates. Both internal standards had a recovery of >80%.

The FAA standards were placed into 1.5 ml of methanol/acetonitrile (1:1, v/v) at a concentration of 5 µM for each compound and injected using the same column, injection volume, and gradient elution as all purified extracts. Once the retention time and *m/z* was confirmed for each identified FAA (Table 3), targeted, MS/MS was completed on each molecule (Table 4) using a 5 µl injection volume and a collision energy (CID) of 15–20 mV.

3 | RESULTS AND DISCUSSION

3.1 | *AANATL2* transcripts are reduced in AANATL2 knockdown offspring

One method for knocking down the expression of AANATL2 in *D. melanogaster* via siRNA is the UAS/Gal4 bipartite approach for targeted gene expression (Duffy, 2002; Kalidas & Smith, 2002). This system employs two different parent mutants to create offspring with targeted gene expression of either native or transposed genes (Brand & Perrimon, 1993). One parent is a mutant containing a chosen responder gene with an activator sequence transposed upstream of transcription that can be bound by the protein, Gal4. This protein, discovered in yeast, is a known transcription activator via its binding to an UAS, which can be transposed into the genome of *D. melanogaster* with no overtly deleterious, phenotypic effects (Giniger et al., 1985). The next parent contains the transposed, functional gene for Gal4 in a predetermined pattern of expression for targeting and is known as the driver. When the two mutants are mated together, the gene of interest in some offspring is rendered under the

TABLE 3 Matching *m/z* and retention times of fatty acid amides detected in the thorax-abdomen

				Retention time (min)		
Fatty acid amides	**Standard (*m/z*)**	**UAS[a] (*m/z*)**	**KD[b] (*m/z*)**	**Standard**	**UAS[a]**	**KD[b]**
N-palmitoyldopamine	392.3164	392.3183	ND	5.998	5.933	ND
N-palmitoylglycine	314.2694	314.2695	314.2690	5.832	5.908	5.830
Palmitamide	256.2640	ND	256.2636	6.040	ND	6.048
Palmitoleamide	254.2483	254.2456	254.2478	5.683	5.667	5.680
N-oleoylethanolamine	326.3064	326.3057	326.3056	5.907	5.909	5.915
Oleamide	282.2797	282.2783	282.2799	6.115	6.116	6.134

Abbreviations: KD, knockdown; ND, not detected; UAS, upstream activator sequence.
[a]UAS parent.
[b]AANATL2 knockdown offspring.

TABLE 4 Tandem mass spectrometry fragmentation of detected fatty acid amides

	Precursor (*m/z*)			Amine (*m/z*)			Acyl (*m/z*)		
Fatty acid amides	**Standard**	**UAS[a]**	**KD[b]**	**Standard**	**UAS[a]**	**KD[b]**	**Standard**	**UAS[a]**	**KD[b]**
Oleamide	282.2785	282.2811	282.2858	100.0752	100.0756	100.0712	135.1136	135.116	135.1175
N-oleoylethanolamine	326.3076	326.3060	326.3055	62.059	62.0605	62.0600	135.1167	135.1164	135.1131
Palmitamide	256.2665	ND	256.2624	100.0742	ND	100.0772	57.0698	ND	57.0687
Palmitoleamide	254.2456	254.2453	254.2522	100.0772	100.0752	100.0759	135.1155	135.1172	135.1166
N-palmitoylglycine	314.2690	314.2880	314.269	76.0397	76.0398	76.0395	57.0700	57.0694	57.0708
N-palmitoyldopamine	392.3160	392.3223	ND	154.0835	154.0856	ND	57.0688	57.0708	ND

Abbreviations: KD, knockdown; ND, not detected; UAS, upstream activator sequence.

[a]UAS parent.

[b]AANATL2 knockdown offspring.

TABLE 5 ΔC_T values calculated for $\Delta\Delta C_T$ analysis

	$C_{T\text{-Actin}}$	$C_{T\text{-AANATL2}}$	ΔC_T
UAS	17.14 ± 0.02	25.82 ± 0.09	8.676 ± 0.09
Knockdown	18.24 ± 0.09	29.45 ± 0.19	11.21 ± 0.21

Abbreviation: UAS, upstream activator sequence.

transcriptional control of the UAS/Gal4 combination in the same expression pattern defined by the Gal4 driver. Furthermore, offspring with targeted gene expression can be differentiated based on the negative selection of a visible, inheritable phenotype from a balancer chromosome in the Gal4 driver (Duffy, 2002).

To use the UAS/Gal4 to successfully knockdown AANATL2, mutant *D. melanogaster* housing a transposed, synthetic gene for an inverted-repeat, hairpin mRNA precursor containing complementary nucleotides to the AANATL2 transcript, the UAS, and short double-stranded RNA stem-loops were obtained. Because the precise cellular location of *N*-acylarylalkylamide biosynthesis is unknown in *D. melanogaster*, a Gal4 driver for ubiquitous expression was chosen to increase the probability of AANATL2 knockdown. Confirmation of AANATL2 knockdown was necessary before measuring any corresponding alterations in the *D. melanogaster* fatty acid amidome.

The fold change of the *AANATL2* transcripts was determined by $\Delta\Delta C_T$ analysis by RT-qPCR in the AANATL2 knockdown offspring of the UAS/Gal4 cross. The cycle threshold (C_T) values recorded for both the AANATL2 target and actin-42A endogenous control for both the UAS parent and knockdown offspring are shown in Table 5. The average C_T values of three replicates for the actin-42A and AANATL2 amplicons in both the UAS parent and AANATL2 knockdown offspring are also included in Table 5. C_T values reflect the amplification of a single product, as there was no amplification detected in the "no-RT" and "no-template," negative controls. All sequencing results came back positive for the appropriate amplicon. The $\Delta\Delta C_T$ is used to find the change in abundance of a target amplicon (*AANATL2*) relative to an endogenous control gene (*actin-42A*). This value is

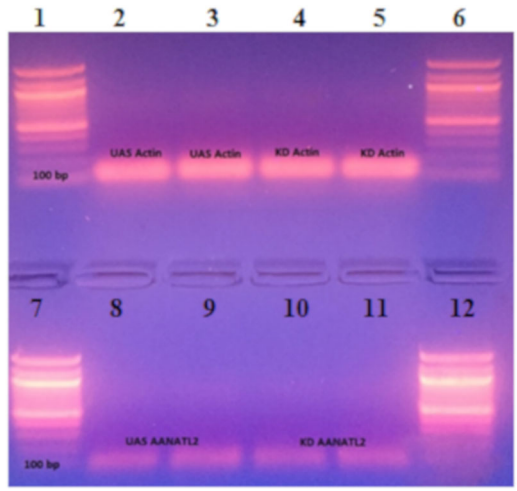

FIGURE 2 Agarose gel of the cDNA Products from RT-qPCR. The cDNA products were analyzed using a 1.8% agarose gel. Lanes 1, 6, 7, and 12 each contain 11 μl of 100 bp ladder (NEB). Lanes 2 and 3 show the actin amplicons of the UAS parents, while lanes 4 and 5 show the actin amplicons for the AANATL2 knockdowns. Lanes 8 and 9 show the AANATL2 amplicons from the UAS parent, while lanes 10 and 11 show the AANATL2 amplicons from the knockdown flies. All actin and AANATL2 amplicons are the correct product sizes, within experimental error (actin = 123 bp and ANATL2 = 120 bp). All excised bands were of the correct matching sequences via sequencing by Eurofins Genomics. AANATL2, aryalkylamine *N*-acetyltransferase-like 2; cDNA, complementary DNA; RT-qPCR, reverse transcription quantitative polymerase chain reaction; UAS, upstream activator sequence

calculated by subtracting the ΔC_T of the UAS from that of the knockdown, yielding a $\Delta\Delta C_T$ value of 2.54 ± 0.23. The fold change in expression of the *AANATL2* transcripts, $2^{-\Delta\Delta C_T} = 2^{-2.54}$, is 0.15–0.20 in the knockdown compared with the UAS parent. In other words, the *AANATL2* transcripts are 80–85% reduced in the offspring when compared with the UAS parent. These data convey the effectiveness of the UAS/Gal4 mating cross to significantly lower levels of *AANATL2* mRNA. The qPCR amplicons are of the expected size, 120 bp for *AANATL2* and 123 bp for *actin-42A* (Figure 2), and were of the appropriate sequence, determined after extracting the DNA from the gels.

3.2 | *Drosophila* AANATL2 protein abundance is reduced in knockdown offspring

Often, transcript levels do not directly correlate with the cellular levels of the corresponding translated protein. We addressed this possibility by comparing the AANATL2 levels between the UAS parents versus the knockdown offspring by western blot analysis. The molecular weight of *D. melanogaster* AANATL2 is 24.3 kDa while that of the His_6-tagged version including the linker sequence between the His_6-tag and the N-terminus of the protein expressed *Escherichia coli* is approximately 2 kDa higher (Dempsey et al., 2014). Thus, the band for endogenous AANATL2 in our western blots would appear below the band for the recombinant AANATL2 control. The western blot of the UAS versus the knockdown offspring shows reduced expression of AAANTL2 in the knockdown offspring (non-Sb[1]) of the UAS/Gal4 (Figure 3). The intensity of the AANATL2 band in the knockdown is lower than the intensity of the AANATL2 band from the UAS parent. These results show that AANATL2 expression in the thorax-abdomen of the knockdown offspring is not as abundant as AANATL2 expression in the thorax-abdomen of the UAS parent and is consistent with the 80–85% reduction in AANATL2 transcript levels as shown by RT-qPCR. Taken together, the RT-qPCR and western blot analysis data confirm the UAS/Gal4 bipartite approach was successful in generating a mutant *D. melanogaster* strain with reduced expression of AANATL2. Knockdown of AANATL2 was not lethal in *D. melanogaster*. In fact, no obvious phenotype was observed in the flies expressing only 15–20% of the wildtype levels of AANATL2, relative to the wildtype (the UAS parent strain).

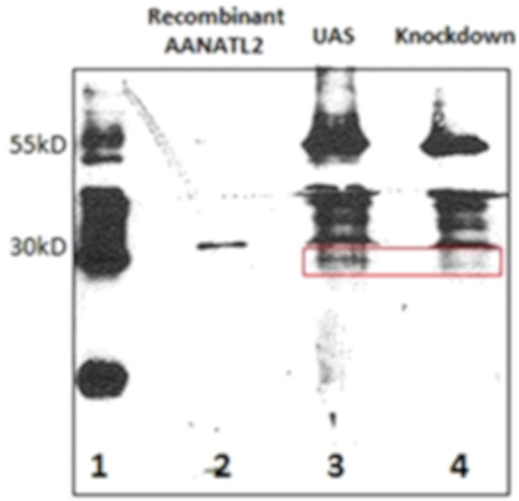

FIGURE 3 AANATL2 knockdown western blot. Proteins were extracted from the thorax-abdomen of the AANATL2 knockdowns and UAS parents. Lane 1 shows the Magic Marker protein ladder. Lane 2 represents a positive control of recombinant AANATL2 (produced in *Escherichia coli*) containing an N-terminal His_6-tag. Lane 3 shows 22 μg of total protein from the thorax-abdomen of the UAS parent and lane 4 shows 22 μg of total protein from the thorax-abdomen of the AANATL2 knockdown offspring. The bands outlined are those for AANATL2 at approximately 25 kDa. AANATL2, aryalkylamine *N*-acetyltransferase-like 2; UAS, upstream activator sequence

TABLE 6 Quantification of fatty acid amides in AANATL2 knockdown *Drosophila melanogaster*

Fatty acid amides	UAS (pmole/g)[a]	AANATL2 KD (pmole/g)[b]
N-palmitoyldopamine	3.5 ± 1.3	ND
N-palmitoylglycine	13 ± 1.7	21 ± 7.5
Palmitamide	ND	4.9 ± 1.2
Palmitoleamide	19 ± 7.8	37 ± 10
N-oleoylethanolamine	37 ± 8.6	14 ± 3.9
Oleamide	32 ± 1.3	370 ± 57

Abbreviations: AANATL2, aryalkylamine *N*-acetyltransferase-like 2; KD, knockdown; ND, not detected; UAS, upstream activator sequence.
[a]Triplicate UAS parent.
[b]Triplicate AANATL2 knockdown offspring.

3.3 | Identification of FAAs in UAS parent and AANATL2 knockdown flies

We found that AANATL2 was only expressed in the thorax-abdomen of *D. melanogaster* (Dempsey et al., 2014); thus, we focused our search for FAAs in the thorax-abdomen. After triplicate LC-QToF-MS injections of the six collected samples (three UAS and three knockdown), the resulting total ion chromatograms were scanned for *m/z* and retention time values matching that of pure, FAA standards. This lead to identification of a set of endogenous FAAs in the thorax-abdomen of the UAS parent and AANATL2 knockdown flies (Table 6). The FAAs identified in the thorax-abdomen of the UAS parent and AANATL2 knockdown flies are similar to, but not identical, with those we reported earlier in a different strain of *D. melanogaster* (Jeffries et al., 2014). Different FAAs were reported in another study in *D. melanogaster* (Tortoriello et al., 2013), also in a different strain of flies, highlighting the strain differences of the fatty acid amidome. Not enough is currently known about the enzymes of FAA biosynthesis and degradation and any strain differences in the expression of these enzymes to explain the observed strain differences in the identified FAAs.

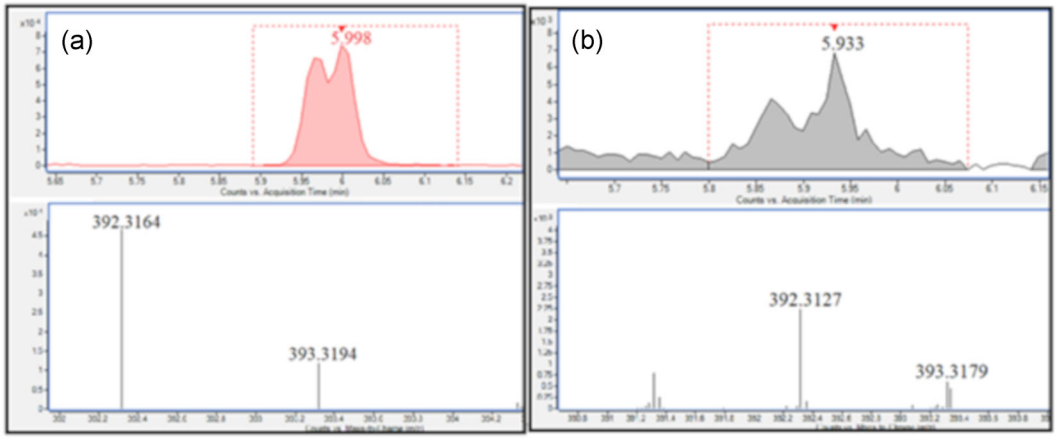

FIGURE 4 Detection of PALDA in the UAS Parent. The top of (a) shows the EIC for PALDA, which has a retention time of 5.998 min. The respective mass spectra for standard PALDA can be seen at the bottom of (a), and depicts an M + 1 of 392.3164 *m/z*. The top of (b) shows the EIC for PALDA in the UAS parent, purified extract, which has a retention time of 5.933 min and an *m/z* of 392.3127 min. There were no significant peaks found in the EIC for the knockdown offspring. EIC, extracted ion chromatogram; PALDA, *N*-palmitoyldopamine; UAS, upstream activator sequence

The differences between the data reported here and those we reported earlier might also result from dietary differences. The flies in our two studies were fed the same commercial food, but different lots of the food were used over the course of our work. Small lot-to-lot variations could contribute to the differences in the fatty acid amidome between our studies.

A consideration of the FAA data of Table 6 within the context of the substrate specificity of AANATL2 is as follows: palmitoyl-CoA, oleoyl-CoA, dopamine, and ethanolamine are AANATL2 substrates, while glycine and ammonia are not (Dempsey et al., 2014, 2015). Consistent with the substrate specificity of AANATL2, we found that the knockdown of AANATL2 resulted in decreased levels of PALDA (Figure 4) and *N*-oleoylethanolamine. In fact, we found no detectable PALDA in the knockdown offspring (Table 6). These data provide strong evidence that AANATL2 does have a role in FAA biosynthesis in *D. melanogaster*, consistent with in vitro substrate specificity studies of the purified enzyme (Dempsey et al., 2014, 2015), and our data showing that the expression pattern of AANATL2 in *D. melanogaster* corresponds to the tissues possessing high levels of endogenous FAAs (Jeffries et al., 2014).

Also found in the AANATL2 knockdown flies were higher levels of *N*-palmitoyl-derived FAAs, *N*-palmitoylglycine, palmitamide, and palmitoleamide (Table 6), relative to the UAS parent. These results suggest that a decrease of PALDA enables a greater flux of the palmitoyl moiety into the other *N*-palmitoylated amines (presumably via an increase in palmitoyl-CoA). A surprising result was the ~10-fold increase in oleamide, increasing from 32 ± 1.3 pmole/g in the USA parent to 370 ± 60 pmole/g in the AANATL2 knockdown (Table 6). The increase in oleamide in the thorax-abdomen of the AANATL2 knockdown flies might represent a "rescue" phenomenon, the increase in oleamide replacing the in vivo function of PALDA. The lack of any observable phenotype in the AANAT2 knockdown flies may point toward oleamide serving a backup function for PALDA in *D. melanogaster*. While there is data on the function of oleamide and PALDA in mammals (Farrell & Merkler, 2008), little is known about the function of these FAAs in *Drosophila*. PALDA may regulate the Hedgehog signaling pathway (Khaliullina, Bilgin, Sampaio, Shevchenko, & Eaton, 2015), a pathway linked to cell growth and differentiation in *Drosophila* (Lum & Beachy, 2004), and oleamide binds to the chemosensory protein, CSP-*sg*4, in the desert locust (Tomaselli et al., 2006). More data on the function of PALDA, oleamide, and the other FAAs identified in *Drosophila* (Jeffries et al., 2014; Tortoriello et al., 2013; Yoshinaga et al., 2007) is necessary to address our hypothesis that PALDA and oleamide have overlapping functions in fruit flies.

4 | CONCLUSION

Overall, our work demonstrates the UAS/Gal4 system can be used to engineer *D. melanogaster* expressing significantly lower levels of AANATL2 than the wildtype and provides strong evidence that AANATL2 catalyzes the formation of *N*-fatty acyldopamines in vivo. Knockdown of AANATL2 expression lead to an increase in oleamide and a decrease in PALDA hinting at redundant functions for PALDA and oleamide in *D. melanogaster*, consistent with the lack of phenotypic changes in the AANATL2 knockdown flies.

ACKNOWLEDGEMENTS

This study has been supported, in part, by grants from the University of South Florida (a Creative Scholarship Grant from the College of Arts and Sciences), the Shirley W. and William L. Griffin Charitable Foundation, the National Institute of Drug Abuse at the National Institutes of Health (R03-DA034323) and the National Institute of General Medical Science of the National Institutes of Health (R15-GM107864) to D.J.M. Special thanks to Sydney Balgo for the collection of insect thorax-abdomen.

CONFICTS OF INTERESTS

The authors declare that there are no conflicts of interest.

AUTHOR CONTRIBUTIONS

R. L. A. designed/completed experiments and wrote the manuscript. D. J. W., A. A., and D. H. helped to complete the experiments. D. J. M. conceived and supervised the study and revised the manuscript.

PROTEIN ACCESSION IDS

AANATL2 (*D. melanogaster*), UniProt ID: Q9VMG0.
Actin-42A (*D. melanogaster*), UniProt ID: P02572.
Chemosensory protein CSP-sg4 (*Schistocerca gregaria*), UniProt ID: O76476.
DNAase I (bovine), UniProt ID: P00639.
Gal4 (yeast), UniProt ID: P04386.
Reverse transcriptase (MMLV), UniProt ID: Q83371.

ORCID

David J. Merkler http://orcid.org/0000-0001-6659-0005

REFERENCES

Alborn, H. T., Turlings, T. C. J., Jones, T. H., Stenhagen, G., Loughrin, J. H., & Tumlinson, J. H. (1997). An elicitor of plant volatiles from beet armyworm oral secretion. *Science*, *276*, 945–949.

Amherd, R., Hintermann, E., Walz, D., Affolter, M., & Meyer, U. A. (2000). Purification, cloning, and characterization of a second arylalkylamine *N*-acetyltransferase from *Drosophila melanogaster*. *DNA and Cell Biology*, *19*, 697–705.

Anderson, R. L., Battistini, M. R., Wallis, D. J., Shoji., C., O'Flynn, B. G., Dillashaw, J. E., & Merkler, D. J. (2018). *Bm*-iAANAT and its potential role in fatty acid amide biosynthesis in *Bombyx mori*. *Prostaglandins, Leukotrienes and Essential Fatty Acids*, *135*, 10–17.

Bradford, M. M. (1976). A rapid and sensitive method for the quantitation of microgram quantities of protein utilizing the principle of protein-dye binding. *Analytical Biochemistry*, *72*, 248–254.

Bradshaw, H. B., Lee, S. H., & McHugh, D. (2009). Orphan endogenous lipids and orphan GPCRs: A good match. *Prostaglandins and Other Lipid Mediators*, *89*, 131–134.

Brand, A. H., & Perrimon, N. (1993). Targeted gene expression as a means of altering cell fates and generating dominant phenotypes. *Development*, *118*, 401–415.

Chu, C. J., Huang, S. M., De Petrocellis, L., Bisogno, T., Ewing, S. A., Miller, J. D., … Walker, J. M. (2003). *N*-oleoyldopamine, a novel endogenous capsaicin-like lipid that produces hyperalgesia. *Journal of Biological Chemistry*, *278*, 13633–13639.

Dempsey, D. R., Carpenter, A.-M., Ospina, S. R., & Merkler, D. J. (2015). Probing the chemical mechanism and critical regulatory amino acid residues of *Drosophila melanogaster* arylalkylamine *N*-acyltransferase like 2. *Insect Biochemistry and Molecular Biology*, *66*, 1–12.

Dempsey, D. R., Jeffries, K. A., Anderson, R. L., Carpenter, A.-M., Rodriquez Opsina, S., & Merkler, D. J. (2014). Identification of an arylalkylamine *N*-acyltransferase from *Drosophila melanogaster* that catalyzes the formation of long-chain *N*-acylserotonins. *FEBS Letters*, *588*, 594–599.

Devane, W. A., Dysarz, F. A., III, Johnson, M. R., Melvin, L. S., & Howlett, A. C. (1988). Determination and characterization of a cannabinoid receptor in rat brain. *Molecular Pharmacology*, *34*, 605–613.

Devane, W. A., Hanus, L., Breuer, A., Pertwee, R., Stevenson, L., Griffin, G., … Mechoulam, R. (1992). Isolation and structure of a brain constituent that binds to the cannabinoid receptor. *Science*, *258*, 1946–1949.

Duffy, J. B. (2002). GAL4 system in *Drosophila*: A fly geneticist's Swiss army knife. *Genesis*, *34*, 1–15.

Elphick, M. R., Satou, Y., & Satoh, N. (2003). The invertebrate ancestry of endocannabinoid signalling: An orthologue of vertebrate cannabinoid receptors in the urochordate *Ciona intestinalis*. *Gene*, *302*, 95–101.

Farrell, E. K., & Merkler, D. J. (2008). Biosynthesis, degradation and pharmacological importance of the fatty acid amides. *Drug Discovery Today*, *13*, 558–568.

Fezza, F., Dillwith, J. W., Bisogno, T., Tucker, J. S., Di Marzo, V., & Sauer, J. R. (2003). Endocannabinoids and related fatty acid amides, and their regulation, in the salivary glands of the lone star tick. *Biochimica et Biophysica Acta*, *1633*, 61–67.

Giniger, E., Varnum, S. M., & Ptashne, M. (1985). Specific DNA binding of GAL4, a positive regulatory protein of yeast. *Cell*, *40*, 767–774.

Hauer, D., Schelling, G., Gola, H., Campolongo, P., Morath, J., Roozendaal, B., … Kolassa, I. T. (2013). Plasma concentrations of endocannabinoids and related primary fatty acid amides in patients with post-traumatic stress disorder. *PLOS One*, *8*, e62741.

Holmes, K., Williams, C. M., Chapman, E. A., & Cross, M. J. (2010). Detection of siRNA induced mRNA silencing by RT-qPCR: Considerations for experimental design. *BMC Research Notes*, *3*, 53.

Iannotti, F. A., Di Marzo, V., & Petrosino, S. (2016). Endocannabinoids and endocannabinoid-related mediators: Targets, metabolism and role in neurological disorders. *Progress in Lipid Research*, *62*, 107–128.

Jeffries, K. A., Dempsey, D. R., Behari, A. L., Anderson, R. L., & Merkler, D. J. (2014). *Drosophila melanogaster* as a model system to study long-chain fatty acid amide metabolism *FEBS Letters*, *588*, 1596–1602.

Merkler, D. J., & Leahy, J. W. (2018). Binding-based proteomic profiling and the fatty acid amides. *Trends in Research*, *1*, https://doi.org/10.15761/TR.1000120

Kalidas, S., & Smith, D. P. (2002). Novel genomic cDNA hybrids produce effective RNA interference in adult *Drosophila*. *Neuron*, *33*, 177–184.

Khaliullina, H., Bilgin, M., Sampaio, J. L., Shevchenko, A., & Eaton, S. (2015). Endocannabinoids are conserved inhibitors of the Hedgehog pathway. *Proceedings of the National Academy of Sciences of the United States of America*, *112*, 3415–3420.

Lum, L., & Beachy, P. A. (2004). The Hedgehog response network: Sensors, switches, and routers. *Science*, *304*, 1755–1759.

McPartland, J., Di Marzo, V., De Petrocellis, L., Mercer, A., & Glass, M. (2001). Cannabinoid receptors are absent in insects. *The Journal of Comparative Neurology*, *436*, 423–429.

Mechoulam, R., Ben-Shabat, S., Hanus, L., Ligumsky, M., Kaminski, N. E., Schatz, A. R., … Vogel, Z. (1995). Identification of an endogenous 2-monoglyceride, present in canine gut, that binds to cannabinoid receptors. *Biochemical Pharmacology*, *50*, 83–90.

Munro, S., Thomas, K. L., & Abu-Shaar, M. (1993). Molecular characterization of a peripheral receptor for cannabinoids. *Nature*, *365*, 61–65.

O'Flynn, B. G., Suarez, G., Hawley, A. J., & Merkler, D. J. (2018). Insect arylalkylamine *N*-acyltransferases: Mechanism and role in fatty acid amide biosynthesis. *Frontiers in Molecular Biosciences*, *5*, 66.

Sugiura, T., Kondo, S., Sukagawa, A., Nakane, S., Shinoda, A., Itoh, K., … Waku., K. (1995). 2-Arachidonoylgylcerol: A possible endogenous cannabinoid receptor ligand in brain. *Biochemical and Biophysical Research Communications*, *215*, 89–97.

Sultana, T., & Johnson, M. E. (2006). Sample preparation and gas chromatography of primary fatty acid amides. *Journal of Chromatography A*, *1101*, 278–285.

Tomaselli, S., Crescenzi, O., Sanfelice, D., Ab, E., Wechselberger, R., Angeli, S., … Picone, D. (2006). Solution structure of a chemosensory protein from the desert locust *Schistocerca gregaria*. *Biochemistry*, *45*, 10606–10613.

Tortoriello, G., Rhodes, B. P., Takacs, S. M., Stuart, J. M., Basnet, A., Raboune, S., … Bradshaw, H. B. (2013). Targeted lipidomics in *Drosophila melanogaster* identifies novel 2-monoacylglycerols and *N*-acyl amides. *PLOS One*, *8*, e67865.

Ud-Din, A. I., Tikhomirova, A., & Roujeinikova, A. (2016). Structure and functional diversity of GCN5-related *N*-acetyltransferases. *International Journal of Molecular Sciences*, *17*, 1018.

Vetting, M. W., De Carvalho, L. P. S., Yu, M., Hegde, S. S., Magnet, S., Roderick, S. L., & Blanchard, J. S. (2005). Structure and functions of the GNAT superfamily of acetyltransferases. *Archives of Biochemistry and Biophysics*, *433*, 212–226.

Walker, J. M., Krey, J. F., Chen, J. S., Vefring, E., Jahnsen, J. A., Bradshaw, H., & Huang, S. M. (2005). Targeted lipidomics: Fatty acid amides and pain modulation. *Prostaglandins and Other Lipid Mediators*, *77*, 35–45.

Witkamp, R. (2016). Fatty acids, endocannabinoids and inflammation. *European Journal of Pharmacology*, *785*, 96–107.

Yoshinaga, N., Aboshi, T., Ishikawa, M., Shimoda, M., Nishida, R., Lait, C. G. … Mori, N. (2007). Fatty acid amides, previously identified in caterpillars, found in the cricket *Teleogryllus taiwanemma* and *Drosophila melanogaster* larvae. *Journal of Chemical Ecology*, *33*, 1376–1381.

How to cite this article: Anderson RL, Wallis DJ, Aguirre A, Holliday D, Merkler DJ. Knockdown of arylalkylamine *N*-acetyltransferase-like 2 in *Drosophila melanogaster*. *Arch. Insect Biochem. Physiol.* 2019;e21608. https://doi.org/10.1002/arch.21608